

Kernel Random Projection Depth for Outlier Detection

Akira Tamamori

Department of Information Science, Aichi Institute of Technology, Aichi, Japan

E-mail: akira-tamamori@aitech.ac.jp

Abstract—This paper proposes an extension of Random Projection Depth (RPD) to cope with multiple modalities and non-convexity on data clouds. In the framework of the proposed method, the RPD is computed in a reproducing kernel Hilbert space. With the help of kernel principal component analysis, we expect that the proposed method can cope with the above multiple modalities and non-convexity. The experimental results demonstrate that the proposed method outperforms RPD and is comparable to other existing detection models on benchmark datasets regarding Area Under the Curves (AUCs) of Receiver Operating Characteristic (ROC).

I. INTRODUCTION

Outlier detection refers to “the problem of finding patterns in data that do not conform to expected normal behavior” [1]. Outlier detection has broad applicability and many application examples, such as fraud detection, intrusion detection, disease detection, medical diagnosis, etc. In supervised learning of classification problems, the authors have reported that utilizing outlier detection for data cleaning, i.e., removing anomalous samples as a preprocessing step, significantly improves the classification accuracy [2]. Accordingly, outlier detection is one of the important research topics in the field of data mining and machine learning.

Outlier detection algorithms often quantify the *outlyingness* (outlierness) of points on a data cloud in a multidimensional space. The opposite of outlyingness is the depth [3]. It measures the centrality of a data point, which defines how close the point is to the center of the data cloud. In other words, the depth introduces a center-outward ordering to the data cloud. Since we can construct analogs of quantiles and ranks in multidimensional datasets from the depth, many authors successfully have applied the depth function in related research fields, such as robust estimation [4], nonparametric tests [5], cluster analysis [6], discriminant analysis [7], multivariate density estimation [8], functional data analysis [9], etc. Authors proposed various depth functions in the literature listed as follows: halfspace depth [10], simplicial volume depth [11], zonoid depth [12], spatial depth [13], projection depth [3, 14], Mahalanobis depth [3, 15], and so on. Among these depth functions, it is known that the halfspace depth and projection depth are favorable since they satisfy the desirable properties of the statistical depth [3]; affine invariance, maximality at the center, monotonicity on rays, null at infinity, etc. We also focus on the projection depth in this study because of these desirable properties. Furthermore, authors in the previous work studied an extension of the spatial depth-based outlier

detection with kernel method [16]. The other study proposed an extension of Mahalanobis depth in the reproducing kernel Hilbert space [17]. Their studies are also related to ours because we consider an extension of the projection depth with the kernel method for outlier detection. In the following, we will describe our motivation in detail.

We have examined the performance of outlier detection methods based on Random Projection Outlyingness (RPO). The detection performance will degrade when data samples are not linearly separable, and the sample distribution exhibits multiple modalities. To cope with the such modalities, we have proposed the RPO-based detection method with a local score weighting [18]. However, the detection performance still needs to improve since it cannot cope with a nonlinearly separable data cloud. The RPO involves inner product computations, i.e., linear operations in the original feature space. In contrast, kernel-based detection methods such as One-Class Support Vector Machine (OCSVM) [19] can deal with such nonlinearly separable distributions using a feature map into Reproducing Kernel Hilbert Space (RKHS), and the kernel function induces the inner product in the RKHS. Combining kernel methods and projection depth will open the possibility of coping with nonlinear separability.

Given a large amount of training data available, we can use detection methods based on deep learning, such as Deep Support Vector Data Description (Deep SVDD) [20] and Deep AutoEncoding Gaussian Mixture Model [21]. These methods first perform a nonlinear mapping which maps the original features into a new feature space, and the detector is trained on the new space. Especially concerning RPO, Deep RPO [22] has been proposed; it combines Deep SVDD and RPO in the training objective. The authors demonstrated that it could improve detection performance than Deep SVDD and RPO. However, training such models on a small dataset will be challenging because sufficient data samples are only sometimes available.

This study proposes an outlier detection method based on Kernel Random Projection Depth (KRPD). A reproducing kernel function maps original feature vectors into the RKHS, and we can compute RPD on the RKHS. Although authors have proposed several methods to obtain a nonlinear mapping related to kernel approximation [23, 24], we adopt Kernel Principal Component Analysis (KPCA) to reduce the dimensionality of the feature vector. This dimensionality reduction helps make the algorithm feasible and avoids the curse of

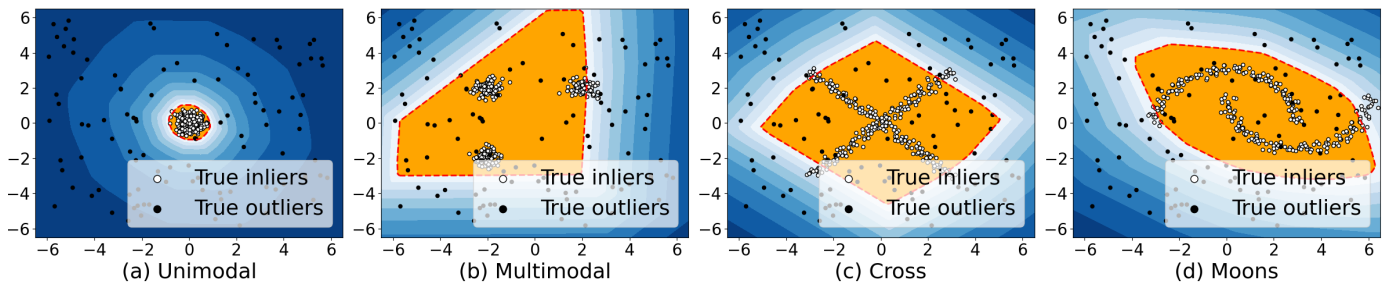


Fig. 1. Contour plots of RPD. The decision boundary is indicated by the red dot line and the central region is colored orange.

dimensionality related to the computations of an inner product in the RKHS. We conducted experiments on benchmark datasets for outlier detection. The results demonstrated that the proposed method outperformed RPD and performed better than other competitive detection methods, including OCSVM, Local Outlier Factor [25], Isolation Forest [26], and Gaussian Mixture Model [27], in terms of Area Under the Curves (AUCs) of Receiver Operating Characteristic (ROC).

II. RANDOM PROJECTION DEPTH

Suppose we are given a d -variate probability distribution P and a data cloud consisting of N data samples

$$X = \{\mathbf{x}_1, \mathbf{x}_2, \dots, \mathbf{x}_N\}, \quad \mathbf{x}_n \sim P, \quad \mathbf{x}_n \in \mathbb{R}^d. \quad (1)$$

Random Projection Outlyingness (RPO) $O_d(\mathbf{x} | X)$ on X is defined as

$$O_d(\mathbf{x} | X) := \sup_{\mathbf{u} \in \mathbb{S}^{d-1}} \frac{|\mathbf{u}^T \mathbf{x} - \text{MED}(\mathbf{u}^T X)|}{\text{MAD}(\mathbf{u}^T X)}, \quad (2)$$

where $\mathbf{x} \in \mathbb{R}^d$ is a d -dimensional data point and \mathbf{u} is a random unit vector drawn from the unit hypersphere \mathbb{S}^{d-1} . The one-dimensional, scalar-valued dataset $\mathbf{u}^T X$ is given by $\mathbf{u}^T X = \{\mathbf{u}^T \mathbf{x}_1, \mathbf{u}^T \mathbf{x}_2, \dots, \mathbf{u}^T \mathbf{x}_N\}$. The abbreviations MED and MAD denote the median and the median absolute deviation, respectively. In accordance with the above definition, we can define Random Projection Depth (RPD) $D_d(\mathbf{x} | X)$ [28] as

$$D_d(\mathbf{x} | X) := \frac{1}{1 + O_d(\mathbf{x} | X)}. \quad (3)$$

Generally, the depth function is a statistic that gives a center-outward ordering to each data point \mathbf{x} . The point at which the depth function takes its maximum value is the median, a *deepest* point. RPD has the characteristic of not being able to deal with multimodal distributions. When we utilize RPD for outlier detection, this characteristic will likely decrease detection accuracy and robustness. To address this problem, we have proposed a method of weighting the outlyingness based on the cardinality of the clusters to which the samples belong [18]. However, this method requires the number of clusters to be determined in advance. Another characteristic of RPD is that the central region forms a convex hull, which also causes an increase in false positive errors when the data cloud is non-convex.

In order to demonstrate the above issues of RPD, we show contour plots and decision surfaces across synthetic datasets in Figure 1. In this figure, datasets are: (a) Unimodal, (b) Multimodal, (c) Cross, and (d) Moons. We generated each dataset with 400 samples (300 inliers, 100 outliers) in two-dimensional space. The true outlier samples were generated by a uniform distribution within $[-6, 6] \times [-6, 6]$. For Unimodal, the inlier samples were generated by a scaled standard normal distributions where the scale was set to 0.3. For Multimodal, the inlier samples were generated by three scaled standard normal distributions. The scale of each normal distribution was also the same value as 0.3. We generated inliers for Cross on the two vertical segments and Moons on the shifted semicircles. Small noises were added to those inliers; the strength of noise was set to 0.05 uniformly.

In this study, we utilize a negative projection depth as the outlier score; a high-depth value corresponds to an inlier, and a low-depth value corresponds to an outlier. We can identify a data point as an outlier if its outlier score is greater than a threshold [16]. The threshold was determined as 25 ($= 100 \times 100/400$) percentile within whole predicted scores. We specify the central region as a set of points where its outlier score exceeds the threshold. The region is colored orange in the figure. We refer to the boundary of the central region as the decision boundary. The central region should include many inliers and few outliers in practice. On Unimodal, we can see that RPD successfully produces a tight boundary and the decision surface encloses almost all inliers. In this case, we can expect that outlier detection works well. However, on other datasets including Multimodal we can see that RPD fails to form tight decision boundaries to inliers and encloses inliers and many outliers. The false positive errors will increase in such cases.

III. PROPOSED METHOD

We propose to compute RPD in an RKHS to resolve the issues described in the previous section, where RPD-based detection will fail on the multi-modal or not linearly separable data cloud. We refer to RPD in the RKHS as Kernel RPD (KRPD). The kernel method [29] makes the computation of KRPD feasible. In the following, we formulate the proposed method.

Suppose we are given a positive definite real-valued kernel

$$k : \Omega \times \Omega \rightarrow \mathbb{R}, \quad (4)$$

where Ω is a non-empty subset of \mathbb{R}^d . We refer the RKHS induced by k as \mathcal{H}_k and define a feature map

$$\Phi : \Omega \rightarrow \mathcal{H}_k, \mathbf{x} \in \Omega \mapsto k(\cdot, \mathbf{x}). \quad (5)$$

The data cloud X is mapped to the data cloud $\mathcal{F}_k(X)$ on \mathcal{H}_k :

$$\mathcal{F}_k(X) = \{\Phi(\mathbf{x}_1), \Phi(\mathbf{x}_2), \dots, \Phi(\mathbf{x}_N)\} \subset \mathcal{H}_k. \quad (6)$$

We can define the outlyingness $O_k(\mathbf{x} \mid \mathcal{F}_k(X))$ and the projection depth $\mathcal{D}_k(\mathbf{x} \mid \mathcal{F}_k(X))$ on \mathcal{H}_k sequentially as

$$O_k(\mathbf{x} \mid \mathcal{F}_k(X)) := \sup_{\|f\|=1} \frac{|\langle f, \Phi(\mathbf{x}) \rangle - \text{MED}(\langle f, \mathcal{F}_k(X) \rangle)|}{\text{MAD}(\langle f, \mathcal{F}_k(X) \rangle)}, \quad (7)$$

and

$$\mathcal{D}_k(\mathbf{x} \mid \mathcal{F}_k(X)) := \frac{1}{1 + O_k(\mathbf{x} \mid \mathcal{F}_k(X))}, \quad (8)$$

where $\|\cdot\|$ denotes the norm in \mathcal{H}_k . The $\langle f, \mathcal{F}_k(X) \rangle$ is an abbreviation of the scalar-valued data cloud

$$\langle f, \mathcal{F}_k(X) \rangle = \{\langle f, \Phi(\mathbf{x}_1) \rangle, \langle f, \Phi(\mathbf{x}_2) \rangle, \dots, \langle f, \Phi(\mathbf{x}_N) \rangle\}, \quad (9)$$

where $\langle \cdot, \cdot \rangle$ denotes the inner product of \mathcal{H}_k . Through non-linear kernel function k and its feature map, we expect that the projection depth is robust to the distribution with multi modality and non-convexity.

Since the dimensionality of \mathcal{H}_k is not necessarily finite, the unit sphere $\mathcal{S}_k = \{f \in \mathcal{H}_k \mid \|f\| = 1\}$ is generally not a compact set. This leads to the case that the supremum of Eq.(7) cannot be approximated through a sequence of elements in \mathcal{S}_k and the computation of the projection depth becomes infeasible. To derive the computationally feasible algorithm, we resort to the representer theorem [29]. We can assume that an element $f \in \mathcal{S}_k$ belongs to the linear span of $\mathcal{F}_k(X)$:

$$f = \sum_{n=1}^N \alpha_n \Phi(\mathbf{x}_n) = \sum_{n=1}^N \alpha_n k(\cdot, \mathbf{x}_n), \quad (10)$$

where $(\alpha_1, \alpha_2, \dots, \alpha_N) \in \mathbb{R}^N$. The condition $\|f\| = 1$ can be rewritten as

$$\alpha^T \mathbf{K} \alpha = 1, \quad (11)$$

where $\alpha = (\alpha_1, \alpha_2, \dots, \alpha_N)^T$ and \mathbf{K} is the $N \times N$ Gram matrix:

$$\mathbf{K} = \begin{pmatrix} k(\mathbf{x}_1, \mathbf{x}_1) & k(\mathbf{x}_1, \mathbf{x}_2) & \cdots & k(\mathbf{x}_1, \mathbf{x}_N) \\ k(\mathbf{x}_2, \mathbf{x}_1) & k(\mathbf{x}_2, \mathbf{x}_2) & \cdots & k(\mathbf{x}_2, \mathbf{x}_N) \\ \vdots & \vdots & \ddots & \vdots \\ k(\mathbf{x}_N, \mathbf{x}_1) & k(\mathbf{x}_N, \mathbf{x}_2) & \cdots & k(\mathbf{x}_N, \mathbf{x}_N) \end{pmatrix}. \quad (12)$$

We can indeed compute the projection depth approximately in \mathcal{H}_k by sampling α from the hyperellipsoid of $\alpha^T \mathbf{K} \alpha = 1$. However, the inner product between high dimensional vectors suffers from the curse of dimensionality; almost all vectors in a high dimensional space are orthogonal to each other [30, 31]. This characteristic will significantly reduce the efficiency and

Algorithm 1 Computation of outlier score based on KRPD.

Input: Data cloud $X = \{\mathbf{x}_1, \mathbf{x}_2, \dots, \mathbf{x}_N\} \subset \Omega$, kernel function k , dominant dimensionality M , the number of random projection vectors L , and a data point $\mathbf{x} \in \Omega$.

Output: Negative projection depth $-D_M(\beta \mid F(X))$.

- 1: Compute the Gram matrix \mathbf{K} between \mathbf{x} and X , and obtain the centralized matrix \mathbf{K}' from \mathbf{K} [29].
 - 2: Compute principal components $\beta_n \in \mathbb{R}^M$ for each \mathbf{x}_n by solving the eigenvalue problem of \mathbf{K}' , and obtain the new data cloud: $F(X) = \{\beta_1, \beta_2, \dots, \beta_N\}$.
 - 3: Draw a set of L random unit vectors from the unit hypersphere \mathbb{S}^{M-1} : $U = \{\mathbf{u}_1, \mathbf{u}_2, \dots, \mathbf{u}_L\} \subset \mathbb{S}^{M-1}$.
 - 4: Compute the principal component $\beta \in \mathbb{R}^M$ for \mathbf{x} .
 - 5: Compute the projected data cloud $\mathbf{u}_l^T F(X)$ for $1 \leq l \leq L$.
 - 6: **return** $-D_M(\beta \mid F(X))$ in accordance with Eq. (14).
-

accuracy of depth computation. To improve the efficiency and accuracy, we propose to perform a dimensionality reduction by KPCA [32] before computing projection depth. In this paper, we denote the principal dominant components as β for a data point \mathbf{x} and its dimensionality as M . We also denote the new data cloud as $F(X) = \{\beta_1, \beta_2, \dots, \beta_N\}$. By treating β and β_n as new coordinates in \mathbb{R}^M , the projection depth can be computed in the same manner as in \mathbb{R}^M . If setting $M < N$, we can simultaneously achieve a nonlinear dimensionality reduction and a feasible computation of the projection depth. The overall computation algorithm is summarized in Algorithm 1. In the step 5), the projected data cloud $\mathbf{u}_l^T F(X)$ is defined as $\mathbf{u}_l^T F(X) := \{\mathbf{u}_l^T \beta_1, \mathbf{u}_l^T \beta_2, \dots, \mathbf{u}_l^T \beta_N\}$. The projection depth $\mathcal{D}_k(\mathbf{x} \mid \mathcal{F}_k(X))$ is approximated as

$$\mathcal{D}_k(\mathbf{x} \mid \mathcal{F}_k(X)) \approx D_M(\beta \mid F(X)) \quad (13)$$

$$\approx \left(1 + \max_{1 \leq l \leq L} \frac{|\mathbf{u}_l^T \beta - \text{MED}(\mathbf{u}_l^T F(X))|}{\text{MAD}(\mathbf{u}_l^T F(X))} \right)^{-1}. \quad (14)$$

We also utilize a negative projection depth as the outlier score in the same way as RPD. The outlier detection algorithm is also the same.

IV. EXPERIMENTAL EVALUATION

We conducted experiments on toy example data and benchmark datasets to evaluate the detection performance of proposed model. The following detection methods were compared with KRPD:

- k -Nearest Neighbors (k NN) [33]
- Local Outlier Factor (LOF) [25]
- Isolation Forest (IForest) [26]
- One-Class Support Vector Machine (OCSVM) [19]
- Kernel Principal Component Analysis (KPCA) [34]
- Random Projection Depth (RPD) [28]

In this study, RBF kernel function $k(\mathbf{x}, \mathbf{y}) = \exp(-\gamma \|\mathbf{x} - \mathbf{y}\|^2)$ was used for OCSVM, KPCA and KRPD.

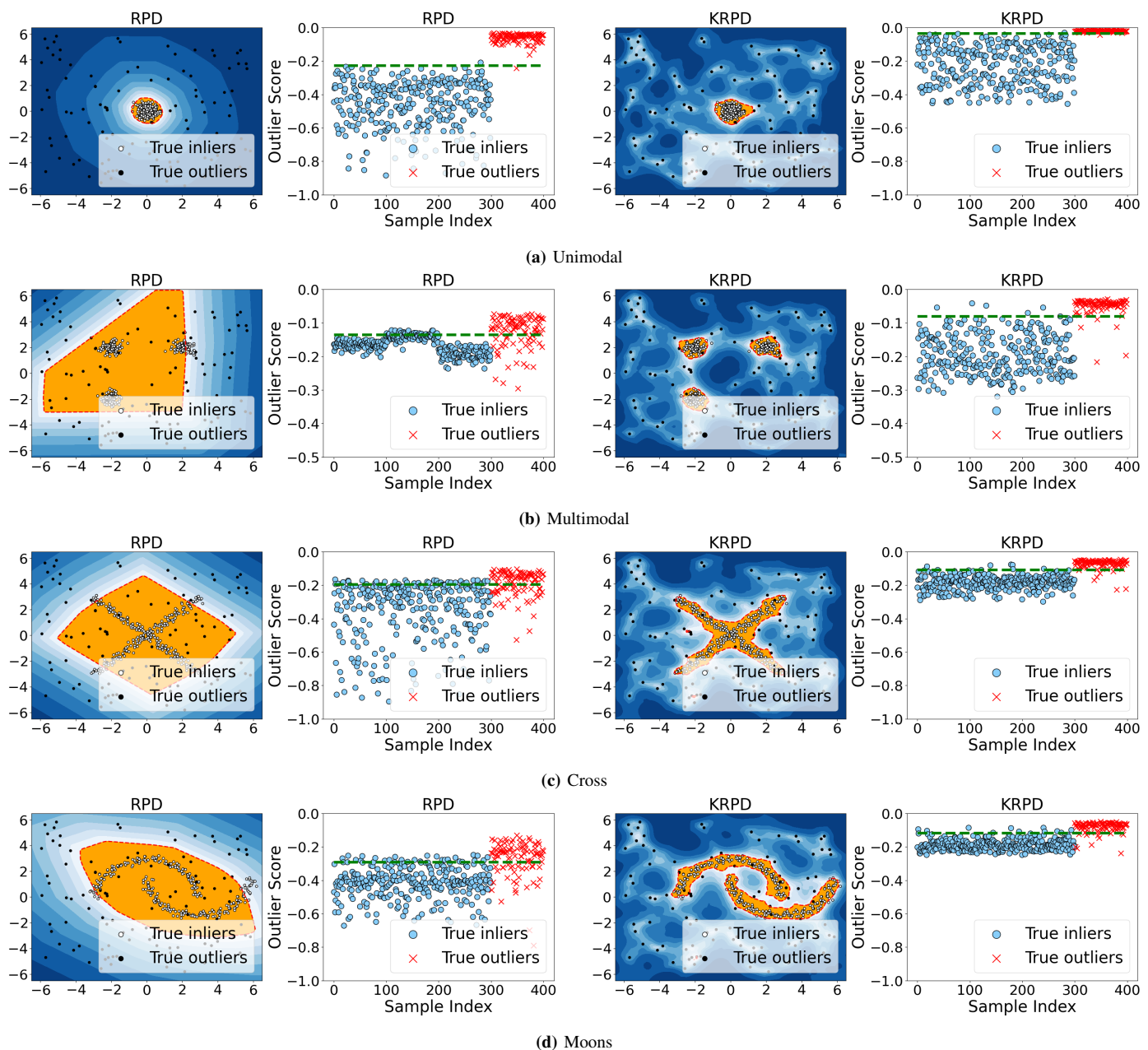


Fig. 2. Contour plots and outlier score comparison between RPD and KRPD. The threshold is indicated by the green dotted line in the outlier score plot. High outlier score corresponds to strong outlyingness.

A. Toy Example

Figure 2 shows contour plot comparisons between RPD and KRPD across toy datasets. We used the same datasets as in Figure 1. We fixed the kernel parameter γ and the dominant dimensionality M to 0.25 and 100, respectively. The threshold of the central region was determined according to the ratio of inliers to the total samples. Namely, the 75 ($= 100 \times 300/400$) percentile of the outlier scores. We also show the outlier scores on each toy data dataset. In these figures, the central region is colored orange and the threshold is represented as the green dotted line. First, we can see that the decision boundaries of

both RPD and KRPD could enclose inliers on the unimodal. It is apparent that the corresponding scores are separated well, and consequently, we obtain few detection errors. Compared with RPD, we can see that the decision boundary of KRPD successfully encloses almost all inlier samples, and many outliers are outside the central region even when the data cloud exhibits multiple modalities and non-convexity. On the multimodal, scores of RPD from several inliers exceed the threshold. Such exceeded scores lead to an increase in false negative detection errors. Furthermore, many scores of RPD from outliers are lower than the threshold, which leads to

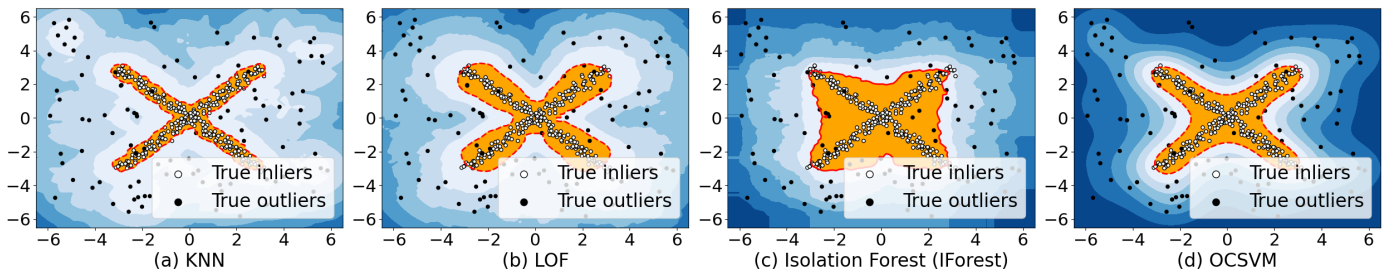


Fig. 3. Contour plots of detection methods on the Cross dataset.

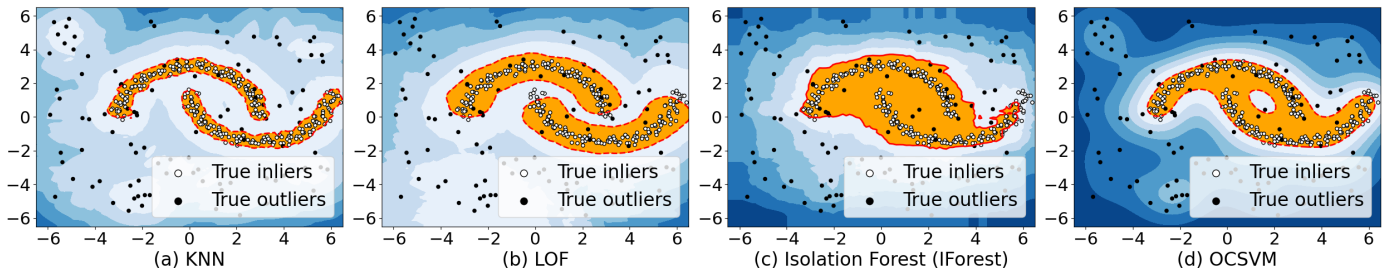


Fig. 4. Contour plots of detection methods on the Moon dataset.

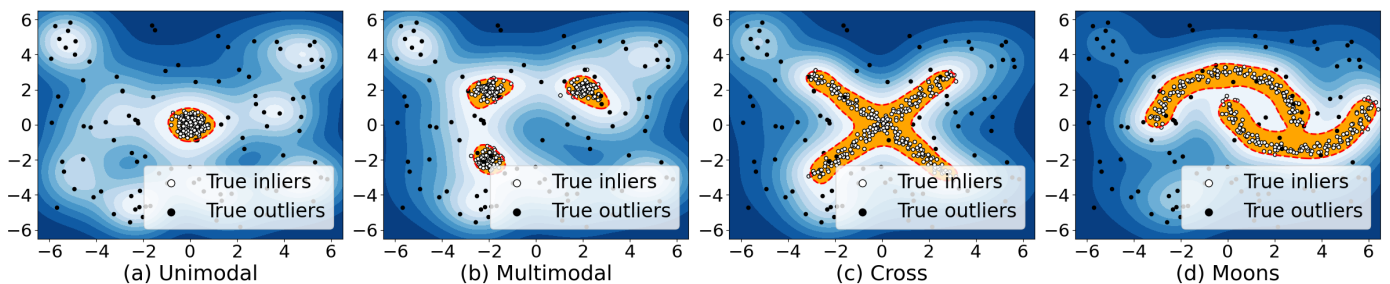


Fig. 5. Contour plots of KPCA-based detector on the toy datasets.

an increase in false positive errors. In contrast, both false positive/negative detection errors decrease in KRPD, as we can see from the right side of the figure. The trend is also generally true for the remaining Cross and Moons. From these results, we can expect that KRPD will demonstrate better detection performance than RPD.

Figure 3 and 4 show the contour plot comparisons on the Cross and Moons dataset, respectively. We can see that the decision boundary of IForest circumscribed the dataset and failed to capture the modalities, which led to an increase in false positive errors. k NN, LOF, and OCSVM achieved tighter boundaries to capture the modalities. Figure 5 shows the contour plots of KPCA on the toy datasets. We applied the same RBF kernel and the hyperparameter γ for both KPCA and KRPD. The dominant dimensionality M was set to 10 for KPCA. In the KPCA-based detection, we used the reconstruction error in the feature space as the outlier score [34]. From the figure, we can see that the boundary fitted the data cloud tightly, and even only KPCA obtained favorable feature spaces for outlier detection. Comparing with

TABLE I
INFORMATION OF BENCHMARK DATASET [35]: DATASET NAME, NUMBER OF SAMPLES, NUMBER OF FEATURE DIMENSIONS, AND OUTLIER PERCENTAGES.

Dataset	#samples	#dims.	outliers (%)
Arrhythmia	452	274	14.6%
Cardio	1831	21	9.61%
Ionosphere	351	33	35.9%
Letter	1600	32	6.25%
MNIST	7603	100	9.21%
Musk	3062	166	3.17%
Optdigits	5216	64	2.88%
Pendigits	6870	16	2.27%
Satellite	6435	36	31.6%
Satimage-2	5803	36	1.22%
Vowels	1456	12	3.43%
Wbc	378	30	5.56%

these figures and Figure 2, we consider that KRPD could achieve the competitive decision boundaries to other methods.

TABLE II
ROC AUC SCORES OF OUTLIER DETECTION METHODS. AVERAGE OF 5 INDEPENDENT TRIALS IS SHOWN. THE BETTER METHOD IS INDICATED IN **BOLD**.

Dataset	kNN	LOF	IForest	OCSVM	KPCA	RPD	KRPD (ours)
Arrhythmia	0.783 ± 0.024	0.774 ± 0.028	0.796 ± 0.040	0.781 ± 0.022	0.768 ± 0.026	0.771 ± 0.021	0.791 ± 0.026
Cardio	0.841 ± 0.018	0.741 ± 0.017	0.928 ± 0.014	0.924 ± 0.012	0.852 ± 0.029	0.936 ± 0.017	0.926 ± 0.015
Ionosphere	0.924 ± 0.016	0.889 ± 0.030	0.839 ± 0.021	0.910 ± 0.017	0.918 ± 0.019	0.866 ± 0.014	0.935 ± 0.012
Letter	0.897 ± 0.011	0.865 ± 0.016	0.614 ± 0.029	0.792 ± 0.028	0.897 ± 0.018	0.617 ± 0.022	0.865 ± 0.018
MNIST	0.872 ± 0.004	0.779 ± 0.008	0.785 ± 0.008	0.859 ± 0.037	0.875 ± 0.004	0.844 ± 0.013	0.856 ± 0.006
Musk	0.972 ± 0.009	0.569 ± 0.028	0.998 ± 0.000	0.836 ± 0.085	0.991 ± 0.011	0.998 ± 0.000	0.997 ± 0.005
Opltdigits	0.394 ± 0.028	0.605 ± 0.080	0.686 ± 0.043	0.528 ± 0.041	0.585 ± 0.053	0.552 ± 0.042	0.755 ± 0.070
Pendigits	0.842 ± 0.005	0.521 ± 0.025	0.950 ± 0.013	0.870 ± 0.038	0.953 ± 0.010	0.838 ± 0.029	0.920 ± 0.008
Satellite	0.717 ± 0.009	0.569 ± 0.007	0.714 ± 0.018	0.715 ± 0.039	0.716 ± 0.007	0.667 ± 0.004	0.727 ± 0.005
Satimage-2	0.992 ± 0.001	0.700 ± 0.057	0.989 ± 0.004	0.963 ± 0.033	0.993 ± 0.004	0.996 ± 0.002	0.994 ± 0.006
Vowels	0.966 ± 0.009	0.934 ± 0.009	0.757 ± 0.040	0.910 ± 0.049	0.940 ± 0.040	0.810 ± 0.049	0.905 ± 0.021
Wbc	0.812 ± 0.026	0.915 ± 0.021	0.937 ± 0.028	0.881 ± 0.062	0.884 ± 0.038	0.911 ± 0.032	0.906 ± 0.012
Average	0.834 ± 0.013	0.738 ± 0.027	0.832 ± 0.022	0.831 ± 0.039	0.864 ± 0.022	0.817 ± 0.020	0.882 ± 0.017

B. Performance Evaluation on Benchmark Datasets

We conducted experiments on twelve standard benchmark datasets publicly available at ODDS library [35] for performance evaluations. The detailed information is listed in Table I. We randomly split each dataset into training and test data in a stratified fashion, specifying a seed; 60% for training and 40% for testing. The outlier percentage was kept the same on both training and test because of the stratified fashion. This split scheme intends to simulate data contamination and evaluate the robustness of the existence of outliers. Moreover, we performed a 5-fold stratified cross-validation on the training data for hyperparameter search. In each fold, 80% of training data were used for actual model training, and the rest of 20% were used for validation.

For both RPD and KRPD, the number of axes L for random projections was fixed to 1000. In order to optimize other hyperparameters, we utilized a framework using the Optuna package [36], which implements a Bayesian optimization. In this framework, we selected a strategy to maximize the ROC AUCs. For OCSVM, KPCA and KRPD, the kernel parameter γ was optimized between $[0.00001, 1.0]$. For both KPCA and KRPD, the number of principal components M was optimized between $[10, 500]$. We can obtain the label information as binary ones because the training data contains inliers and outliers. Hence we could also compute ROC AUCs on each fold of the training data, and the hyperparameters were determined semi-supervised. The Optuna optimized the hyperparameters according to the maximization criterion.

Table II lists ROC AUCs. We can see that KRPD outperformed RPD regarding ROC-AUCs on the nine datasets. Significantly, KRPD greatly improved the detection performance on Letter and Opltdigits datasets. On the three datasets of Cardio, Musk, and Satimage-2, the performance of RPD was almost the same as KRPD. The averaged AUCs of KPCA was 0.864 ± 0.022 , and it was comparable to other detection methods. Although KPCA outperformed KRPD on several datasets, KRPD outperformed KPCA on average, and especially, the improvement was significant on the Opltdigits.

V. DISCUSSION

We have shown in the previous section that KRPD outperformed RPD and was comparable to other detection methods on average. These results demonstrate the effectiveness of KRPD in detecting outliers. However, KRPD did not deliver the best detection performance across all datasets. In this section, we will consider why we obtained variations across datasets in the detection performance of KRPD by using a visualization of datasets. We will also clarify the advantages against other methods and limitations of KRPD.

A. Variations of detection performance across datasets

Figure 6 shows visualizations of Cardio, Letter, Opltdigits, and Satellite datasets by UMAP [37]. As shown in Figure 6a of Cardio, almost outliers locate around the edge of the inlier distribution, and the distribution looks roughly uni-modal. This observation explains why RPD outperformed KRPD slightly. Next, on Letter and Opltdigits, KRPD outperformed RPD significantly. From the corresponding visualization of Letter as shown in Figure 6b, we can observe that roughly three clusters exist, corresponding to three capital letters in the English alphabet. Those clusters are further split into many small groups, and outliers are scattered. The detection with KRPD worked well even in such a challenging dataset. The Opltdigits is a collection of instances of digits 0-9, and digit 0 is the outlier class. We can observe that its data cloud of Opltdigits forms explicit clusters corresponding to each digit, and hence it shows multiple modalities. These observations also explain the superior performance of KRPD to RPD and other methods. As shown in Figure 6d of Satellite, the data cloud of outliers overlaps that of inliers, partly explaining the decrease of AUCs for KRPD. Namely, this decrease explains that KRPD is sensitive to the existence of outliers, that is, contamination in the training data, leading to an increase in the false alarm rate.

B. Detection performance without KPCA

As described in Section III, KPCA is applied to avoid reducing the efficiency and accuracy of depth computation. Hence, a natural question arises: How much will the performance

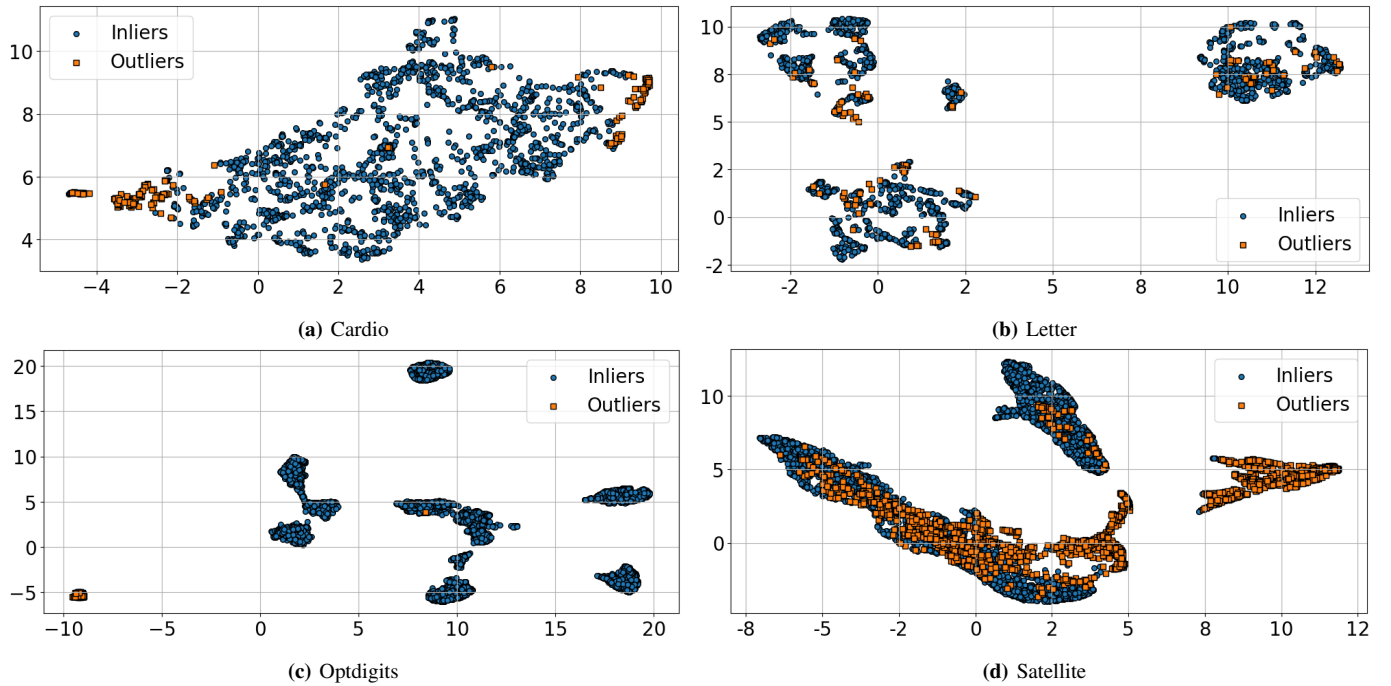


Fig. 6. Visualization of datasets by UMAP.

TABLE III
ROC AUC SCORES OF KRPD W/O AND W/ KPCA. AVERAGE OF 5
INDEPENDENT TRIALS IS SHOWN. THE BETTER METHOD IS INDICATED IN
BOLD.

Dataset	w/o KPCA (RFF)	w/ KPCA
Arrhythmia	0.768 ± 0.033	0.791 ± 0.026
Cardio	0.943 ± 0.015	0.926 ± 0.015
Ionosphere	0.855 ± 0.039	0.935 ± 0.012
Letter	0.618 ± 0.018	0.865 ± 0.018
MNIST	0.820 ± 0.033	0.856 ± 0.006
Musk	0.998 ± 0.002	0.997 ± 0.005
Optdigits	0.543 ± 0.043	0.755 ± 0.070
Pendigits	0.896 ± 0.020	0.920 ± 0.008
Satellite	0.689 ± 0.020	0.727 ± 0.005
Satimage-2	0.996 ± 0.003	0.994 ± 0.006
Vowels	0.787 ± 0.035	0.905 ± 0.021
Wbc	0.896 ± 0.030	0.906 ± 0.012
Average	0.817 ± 0.025	0.882 ± 0.017

degrade without KPCA? We conducted additional experiments to investigate the impact of using or not using KPCA on detection performance. We selected a kernel approximation method with random Fourier features (RFF) [23]. The RFF obtains a high dimensional vector for each \mathbf{x}_n in the data cloud X , and hence we can compute the projection depth. The number of Monte Carlo samples for RFF, corresponding to the dimensionality of the feature vector, was optimized between [10, 500] with the Optuna package. The kernel parameter was also optimized between [0.00001, 1.0].

Table III lists the ROC AUCs of KRPD without and with KPCA. We can see that the average performance significantly decreased without KPCA. We consider that this performance

degradation was due to the curse of dimensionality because RFF involves computations of the inner product in a high dimensional space to approximate the kernel function. As described in Section III, almost all pairs of vectors on a unit hypersphere will become orthogonal. This fact significantly affects the computation of projection depth and partly explains the performance degradation without KPCA.

C. Limitations and future work

Since KRPD inherits advantages from KPCA, it also inherits its limitations. First, careful hyperparameter tuning is often required. In the experimental evaluation, the KRPD hyperparameters could be determined semi-supervised since we had labeled samples available. KRPD will be more effective in semi-supervised situations. Second, KPCA is not necessarily robust to outliers in the training data. Although KPCA has an application of denoising [38], its formulation does not assume the existence of outliers, and the outliers will distort the direction of eigenvectors. Authors in the previous study [39] have proposed several regularization techniques to obtain eigenvectors robustly against outliers. In the future, we will consider an extension of KPCA for RPD to cope with outliers and robust extraction of eigenvectors. Third, the computational complexity is still $O(N^3)$, where N is the number of training samples. Approximate kernel PCA [40] will be effective when N itself becomes a large number, e.g., $N > 10^4$. Kernel PCA with an online learning algorithm [41] will also reduce computational complexity. We will investigate correlations among the number of training samples, the dimensionality of the principal subspace, and its detection performance. Lastly, we have not given statistical support to explain the improved

detection performance from the viewpoint of statistical depth. We are interested in how the desirable properties of statistical depth [3] behave when changing the dimensionality M and the number of training samples N .

VI. CONCLUSION

In this paper, we proposed KRPD, an extension of RPD for outlier detection. The original data cloud is mapped to RKHS by a reproducing kernel function, and we can compute RPD in the RKHS. With the help of KPCA, the decision boundary of KRPD fits the data cloud tightly even when the cloud shows complicated multiple modalities and non-convexity. We evaluated outlier detection performance for RPD, KRPD, and other popular methods on 12 benchmark datasets. The experimental results demonstrated that KRPD outperformed RPD and was comparable to other methods. We also discussed the detection performance between KPCA and KRPD and confirmed that KRPD was more effective than KPCA. We plan to extend KRPD further to utilize robust KPCA.

ACKNOWLEDGMENTS

This work was supported by JSPS KAKENHI Grant Number JP21K17771.

REFERENCES

- [1] V. Chandola and V. Kumar, "Anomaly Detection : A Survey," *ACM Computing Surveys*, vol. 41, Jan. 2009.
- [2] M. R. Smith and T. Martinez, "Improving classification accuracy by identifying and removing instances that should be misclassified," in *The 2011 International Joint Conference on Neural Networks*, 2011, pp. 2690–2697.
- [3] Robert Serfling and Yijun Zuo, "General notions of statistical depth function," *The Annals of Statistics*, vol. 28, no. 2, pp. 461–482, 2000.
- [4] Z. Chen and D. E. Tyler, "On the finite sample breakdown points of redescending m-estimates of location," *Statistics & Probability Letters*, vol. 69, no. 3, pp. 233–242, 2004.
- [5] S. Chenouri and C. G. Small, "A nonparametric multivariate multisample test based on data depth," *Electronic Journal of Statistics*, vol. 6, pp. 760–782, 2012.
- [6] R. Hoberg, "Cluster analysis based on data depth," in *Data Analysis, Classification, and Related Methods*, Berlin, Heidelberg: Springer Berlin Heidelberg, 2000, pp. 17–22.
- [7] A. K. Ghosh and P. Chaudhuri, "On data depth and distribution-free discriminant analysis using separating surfaces," *Bernoulli*, vol. 11, no. 1, pp. 1–27, 2005.
- [8] R. Fraiman, R. Y. Liu, and J. Meloche, "Multivariate density estimation by probing depth," *Lecture Notes-Monograph Series*, vol. 31, pp. 415–430, 1997.
- [9] S. López-Pintado and J. Romo, "On the concept of depth for functional data," *Journal of the American Statistical Association*, vol. 104, no. 486, pp. 718–734, 2009.
- [10] T. J. W., "Mathematics and the picturing of data," *Proceedings of the International Congress of Mathematicians, Vancouver, 1975*, vol. 2, pp. 523–531, 1975.
- [11] H. Oja, "Descriptive statistics for multivariate distributions," *Statistics & Probability Letters*, vol. 1, no. 6, pp. 327–332, 1983.
- [12] G. Koshevoy and K. Mosler, "Zonoid trimming for multivariate distributions," *The Annals of Statistics*, vol. 25, no. 5, pp. 1998–2017, 1997.
- [13] Y. Vardi and C.-H. Zhang, "The multivariate L_1 -median and associated data depth," *Proceedings of the National Academy of Sciences*, vol. 97, no. 4, pp. 1423–1426, 2000.
- [14] R. Y. Liu, "Data depth and multivariate rank tests," *LI-statistical analysis and related methods*, pp. 279–294, 1992.
- [15] P. C. Mahalanobis, "On the generalized distance in statistics," *Proceedings of the National Institute of Sciences (Calcutta)*, vol. 2, pp. 49–55, 1936.
- [16] Y. Chen, X. Dang, H. Peng, and H. Bart, "Outlier Detection with the Kernelized Spatial Depth Function," *IEEE Transactions on Pattern Analysis and Machine Intelligence*, vol. 31, no. 2, pp. 288–305, 2009.
- [17] Y. Hu, Y. Wang, Y. Wu, Q. Li, and C. Hou, "Generalized mahalanobis depth in the reproducing kernel hilbert space," *Statistical Papers*, vol. 52, pp. 511–522, 2011.
- [18] A. Tamamori, "Unsupervised outlier detection based on random projection outlyingness with local score weighting," *IEICE Transactions on Information and Systems*, vol. E106.D, no. 7, 2023, in press.
- [19] B. Schölkopf, J. C. Platt, J. C. Shawe-Taylor, A. J. Smola, and R. C. Williamson, "Estimating the support of a high-dimensional distribution," *Neural Comput.*, vol. 13, no. 7, pp. 1443–1471, 2001.
- [20] L. Ruff *et al.*, "Deep one-class classification," in *Proceedings of the 35th International Conference on Machine Learning*, ser. Proceedings of Machine Learning Research, vol. 80, PMLR, 2018, pp. 4393–4402.
- [21] B. Zong *et al.*, "Deep autoencoding gaussian mixture model for unsupervised anomaly detection," in *International Conference on Learning Representations*, 2018.
- [22] M. Bauw, S. Velasco-Forero, J. Angulo, C. Adnet, and O. Airiau, "Deep random projection outlyingness for unsupervised anomaly detection," *CoRR*, vol. abs/2106.15307, 2021. arXiv: 2106.15307.
- [23] A. Rahimi and B. Recht, "Random features for large-scale kernel machines," in *Advances in Neural Information Processing Systems*, vol. 20, Curran Associates, Inc., 2007.
- [24] C. Williams and M. Seeger, "Using the nyström method to speed up kernel machines," in *Advances in Neural Information Processing Systems*, vol. 13, MIT Press, 2000.
- [25] M. M. Breunig, H.-P. Kriegel, R. T. Ng, and J. Sander, "Lof: Identifying density-based local outliers," in *Proc. of ICMD*, Dallas, Texas, USA, 2000, pp. 93–104.
- [26] F. T. Liu, K. M. Ting, and Z.-H. Zhou, "Isolation forest," in *2008 Eighth IEEE International Conference on Data Mining*, 2008, pp. 413–422.
- [27] O. Barkan and A. Averbuch, "Robust mixture models for anomaly detection," in *Proc. of MLSP*, 2016, pp. 1–6.
- [28] Y. Zuo, "Projection-based depth functions and associated medians," *The Annals of Statistics*, vol. 31, no. 5, pp. 1460–1490, 2003.
- [29] B. Schölkopf and A. J. Smola, *Learning with Kernels: Support Vector Machines, Regularization, Optimization, and Beyond*. The MIT Press, 2018.
- [30] P. Hall, J. S. Marron, and A. Neeman, "Geometric representation of high dimension, low sample size data," *Journal of the Royal Statistical Society: Series B*, vol. 67, no. 3, pp. 427–444, 2005.
- [31] M. Wainwright, *High-Dimensional Statistics: A Non-Asymptotic Viewpoint* (Cambridge Series in Statistical and Probabilistic Mathematics). Cambridge University Press, 2019.
- [32] B. Schölkopf, A. Smola, and K.-R. Müller, "Nonlinear Component Analysis as a Kernel Eigenvalue Problem," *Neural Computation*, vol. 10, no. 5, pp. 1299–1319, 1998.
- [33] F. Angiulli, T. Elomaa, H. Mannila, and H. Toivonen, "Fast outlier detection in high dimensional spaces," in *Proc. of PKDD*, Springer Berlin Heidelberg, 2002, pp. 15–27.
- [34] H. Hoffmann, "Kernel pca for novelty detection," *Pattern Recognition*, vol. 40, no. 3, pp. 863–874, 2007.
- [35] S. Rayana, *Odds library*, <http://odds.cs.stonybrook.edu/>, 2016.
- [36] T. Akiba, S. Sano, T. Yanase, T. Ohta, and M. Koyama, "Optuna: A next-generation hyperparameter optimization framework," in *Proc. KDD*, Anchorage, AK, USA, 2019, pp. 2623–2631.
- [37] L. McInnes and J. Healy, "UMAP: Uniform manifold approximation and projection for dimension reduction," *ArXiv e-prints*, Feb. 2018. arXiv: 1802.03426.
- [38] S. Mika, B. Schölkopf, A. Smola, K.-R. Müller, M. Scholz, and G. Rätsch, "Kernel pca and de-noising in feature spaces," in *Advances in Neural Information Processing Systems*, vol. 11, MIT Press, 1998.
- [39] D. Wang and T. Tanaka, "Robust kernel principal component analysis with $l_{2,1}$ -regularized loss minimization," *IEEE Access*, vol. 8, pp. 81 864–81 875, 2020.
- [40] B. K. Sriperumbudur and N. Sturge, "Approximate kernel pca: Computational versus statistical trade-off," *The Annals of Statistics*, vol. 50, no. 5, pp. 2713–2736, 2022.
- [41] P. Honeine, "Online kernel principal component analysis: A reduced-order model," *IEEE Transactions on Pattern Analysis and Machine Intelligence*, vol. 34, no. 9, pp. 1814–1826, 2012.